

Lawrence Berkeley National Laboratory

Recent Work

Title

MAGNETIC MOMENTS OF THENIUM-186 AND RHENIUM-188 AND ANALYSIS OF THE RHENIUM HYPERFINE STRUCTURE

Permalink

<https://escholarship.org/uc/item/55t96217>

Authors

Armstrong, Lloyd
Marrus, Richard.

Publication Date

1964-11-04

University of California

**Ernest O. Lawrence
Radiation Laboratory**

MAGNETIC MOMENTS OF RHENIUM-186 AND RHENIUM-188
AND ANALYSIS OF THE RHENIUM HYPERFINE STRUCTURE

TWO-WEEK LOAN COPY

*This is a Library Circulating Copy
which may be borrowed for two weeks.
For a personal retention copy, call
Tech. Info. Division, Ext. 5545*

Berkeley, California

DISCLAIMER

This document was prepared as an account of work sponsored by the United States Government. While this document is believed to contain correct information, neither the United States Government nor any agency thereof, nor the Regents of the University of California, nor any of their employees, makes any warranty, express or implied, or assumes any legal responsibility for the accuracy, completeness, or usefulness of any information, apparatus, product, or process disclosed, or represents that its use would not infringe privately owned rights. Reference herein to any specific commercial product, process, or service by its trade name, trademark, manufacturer, or otherwise, does not necessarily constitute or imply its endorsement, recommendation, or favoring by the United States Government or any agency thereof, or the Regents of the University of California. The views and opinions of authors expressed herein do not necessarily state or reflect those of the United States Government or any agency thereof or the Regents of the University of California.

UCRL-11750

UNIVERSITY OF CALIFORNIA

Lawrence Radiation Laboratory
Berkeley, California

AEC Contract No. W-7405-eng-48

**MAGNETIC MOMENTS OF RHENIUM-186 AND RHENIUM-188
AND ANALYSIS OF THE RHENIUM HYPERFINE STRUCTURE**

Lloyd Armstrong, Jr., and Richard Marrus

November 4, 1964

Magnetic Moments of Rhenium-186 and Rhenium-188
and Analysis of the Rhenium Hyperfine Structure

Lloyd Armstrong, Jr., and Richard Marrus

Lawrence Radiation Laboratory and Department of Physics
University of California, Berkeley, California

November 4, 1964

ABSTRACT

The nuclear moments of rhenium-186 and rhenium-188 have been measured by the method of triple resonance in an atomic beam. They are found to be $\mu_I(186) = + 1.728(.003)$ nm and $\mu_I(188) = + 1.777(.005)$ nm, including the correction for diamagnetic shielding. With these values, an analysis based on the wave function of Trees has been undertaken of the hyperfine structure (hfs) in the ${}^6S_{5/2}$ ground state arising from the half-filled 5d shell. Calculations are made of contributions arising from the breakdown of Russell-Saunders coupling within the configuration $(5d)^5(6s)^2$ and configuration mixing by $(5d)^6(6s)$. It is shown that the principal contribution to the magnetic dipole hfs comes from relativistic effects in ${}^6S_{5/2}$. This is consistent with the small value obtained for the hyperfine anomaly ${}^{186}\Delta^{188} = 0.1(0.4)\%$. It is found that if the radial wave functions of Cohen for 5d electrons are used to calculate relativistic corrections, then good agreement is obtained with the measured A constant. The correction factors of Casimir are shown to be too small by a factor of four.

The quadrupole hyperfine structure is found to arise primarily from the cancellation of two off-diagonal matrix elements: a nonrelativistic element $\langle {}^4P_{5/2} | q_J | {}^4D_{5/2} \rangle$ and a relativistic element $\langle {}^6S_{5/2} | q_J | {}^4P_{5/2} \rangle$.

Unfortunately, the accuracy is insufficient to permit a reliable determination of even the sign of the quadrupole moment.

The measured nuclear moments are compared with the predictions of the Nilsson model. Good agreement is found if free-nucleon g factors are used, and excellent agreement is obtained with quenched g factors.

INTRODUCTION

The research reported herein was undertaken for several reasons. First, we hoped to demonstrate that the triple resonance method could be applied to radioactive nuclei with sufficient signal-to-noise ratio so that it can be regarded as a generally applicable technique for the direct determination of magnetic moments. Second, the source of hyperfine structure in systems with half-filled closed electronic shells is a subject of considerable interest. It is therefore important to extend our experimental knowledge to the case of rhenium, for which the ground state is ${}^6S_{5/2}$ arising from $(5d)^5(6s)^2$. Third, the rhenium nuclei lie in a region of intermediate deformation on the basis of the Nilsson model and it is desirable to know if the model is still useful in understanding the properties of these nuclei.

Prior to this research, much work had been done to clarify the electronic and nuclear structure of the ground state. Optical spectroscopy showed the ground state to be ${}^6S_{5/2}$, arising from $(5d)^5(6s)^2$, with a measured g_J factor of - 1.950.¹ The entire optical spectrum of ReI was subjected to theoretical analysis by Trees.² This analysis includes effects due to the breakdown of Russell-Saunders coupling within the configuration $(5d)^5(6s)^2$ and admixing of the configuration $(5d)^6(6s)$. The Trees analysis reproduces the energy-level spectrum to within 1%. We will show that it can also predict both the magnetic dipole and electric quadrupole hfs provided relativistic effects are included. Subsequent atomic beams work showed that the nuclear spins were $I = 1$,³ in agreement with determinations by nuclear spectroscopists from the beta decay. Recently the hyperfine-structure constants of these isotopes were also measured.⁴

Relevant measurements have also been made on one of the stable isotopes, rhenium-185. The nuclear moment of this isotope has been determined by NMR to be $\mu_I(185) = + 3.144 \text{ nm}$.⁵ An optical spectroscopic measurement of the hfs in this isotope has recently been reported, and shows that $A(185) = - 72(24) \text{ Mc}$.⁶ With these measurements the sign of the magnetic moment unambiguously determines the sign of the magnetic dipole constant for any other rhenium isotope.

METHOD, OBSERVATIONS, AND DATA FITTING

The basic method employed is the atomic-beam flop-in method of Zacharias. For details of the application to radioactive atoms the reader is referred to the many review articles on the subject.⁷ The method of beam production is the wire-bombardment technique reported previously.³ Rhenium wires of 20-mil diameter were irradiated at the GETR at Vallecitos and at the MTR in Idaho. Bombardment times were 4 hours for the 17-hour isotope and 3 days for the 90-hour isotope. Under these conditions stable beams are obtainable which last for many hours of running. Detection of the radioactive rhenium is by collection on freshly flamed platinum surfaces and subsequent counting in low-background beta counters (about 1 cpm).

The triple resonance method has been described previously.⁸ For application to the rhenium isotopes, three shorted coaxial hairpins were placed in the C-magnet region. The hairpins are about 0.5 in. long, and the spacing between them is about 1.5 in. The C-magnet pole tips are parallel hypernom plates with 0.5 in. separation. A schematic of the hairpin arrangement is shown in Fig. 1.

The following procedure was used in searching for resonances. The A hairpin was set on a flop-in transition of the type $\Delta F = 0$, $\Delta m_F = \pm 1$, and the single-loop hairpin signal maximized. A signal-to-noise ratio of about 10:1 could be obtained. The B hairpin was then set for resonance on the same transition and the flop-in signal was minimized. The reduced signal was generally not much above machine background. With fixed frequencies in the A and B hairpins, the frequency in the C hairpin was varied. In this way we searched for resonances in transitions which in high field are describable by $\Delta m_J = 0$, $\Delta m_I = \pm 1$. Resonance is indicated by an increased signal at the detector and signal-to-noise ratios as high as the single-loop ratio could be obtained. At the highest fields (500 gauss) line widths for the A and B resonances were about 400 kc, whereas the triple-resonance line was only about 25 kc wide. Some of the observed triple-resonance lines are shown in Fig. 2.

In Fig. 3 we give a schematic of the hyperfine structure of both rhenium isotopes. The flop-in transitions observed in the A and B hairpins are labeled by α , β , and γ , and the C hairpin transitions are denoted by numbers. In Table I all the observations are tabulated.

Data fitting was done in the following way. Our data were combined with those of Schlecht et al.⁴ and all the observations fitted to a Hamiltonian of the form

$$\mathcal{H} = A\bar{I}\cdot\bar{J} + \frac{B}{2IJ(2I-1)(2J-1)} [3(\bar{I}\cdot\bar{J})^2 + 3/2(\bar{I}\cdot\bar{J}) - I(I+1)J(J+1)] \\ - g_J\mu_0\bar{J}\cdot\bar{H} - g_I\mu_0\bar{I}\cdot\bar{H}$$

This fit was accomplished by means of an IBM 7090 program in which A, B, g_J , and g_I are treated as free parameters. The final results are,

for Re^{186} : $A = - 78.3060(10) \text{ Mc/sec}$,

$B = + 8.3595(16) \text{ Mc/sec}$,

$g_J = - 1.951988(39)$,

$g_I = 9.34(2) \times 10^{-4}$;

for Re^{188} : $A = - 80.4326(8) \text{ Mc/sec}$,

$B = + 7.7463(11) \text{ Mc/sec}$,

$g_J = - 1.952072(60)$,

$g_I = 9.61(3) \times 10^{-4}$.

The sign of A is determined from the measured sign of g_I and Winkler's results⁶ on stable Re^{185} , which show that for positive g_I negative A obtains.

The sign of B is determined from the sign of A and the measured B/A ratio, which is negative. From these results the hyperfine anomaly can be obtained directly. We find

$${}^{186}\Delta^{188} \equiv \frac{A^{186}/A^{188}}{g_I^{186}/g_I^{188}} - 1 = 0.1(0.4)\%.$$

The values obtained for g_I must be corrected for the diamagnetic shielding effect.⁹ We write, in the usual way,

$$g_I = g_I^{\text{screened}} \frac{1}{1 - \sigma},$$

and use for σ the value 1.00714 appropriate to $Z = 64$. This gives

$g_I(186) = 9.41(2) \times 10^{-4}$ and $g_I(188) = 9.68(3) \times 10^{-4}$, and for the nuclear moments $\mu_I(186) = 1.728(3) \text{ nm}$ and $\mu_I(188) = 1.777(5) \text{ nm}$.

Since the g_J values obtained for the two isotopes should be the same, a weighted mean may be taken. We get $g_J({}^6S_{5/2}) = -1.952021(33)$. This value can be compared with the value predicted by Trees' wave function of -1.946. The discrepancy is of the right order and sign, so that it is probably due to relativistic effects.

The comparison between our results and the theoretical values obtained with this fit is given in Table I. It should be mentioned that it is

the data of Schlecht et al. that essentially fix A, B, and g_J . The triple-resonance results cause only minor variations in these values but serve to fix g_I precisely.

Since the g_I term in the Hamiltonian is smaller by several orders of magnitude than the other terms, it is important to ask if there are systematic effects which contribute to g_I . We may write this term as $-g_I(1 + \alpha)\mu_0 \bar{I} \cdot \bar{H}$, where g_I is the "true" nuclear g factor and α arises from systematic effects. There are two possible mechanisms we have considered.

(a) Electronic perturbations: Such effects arise from mixing into the ground state of other electronic states in such a way as to introduce a pseudo $\bar{I} \cdot \bar{H}$ term. A perturbation calculation shows that the order of magnitude is less than 10^{-4} .

(b) Effects proportional to the magnetic field: This would occur, for example, if the magnetic field seen by the radioactive beam is different from the field at the calibrating beam. This particular mechanism is also found to be less than 10^{-4} . Further evidence that these effects are small comes from the g_J value. If the particular mechanism were different in the two isotopes we would expect it to give rise to different g_J for the two isotopes. The agreement of the two g_J values to within 10^{-5} suggests that these effects are small.

Finally, a term which cannot be written in the above form would show up in the χ^2 reflecting the goodness of fit. For our experiment, χ^2 is small enough to suggest that the assigned errors are conservative.

HYPERFINE FIELDS

We now examine the possible mechanisms by which the hyperfine fields in the rhenium atom could be established. The magnetic field at the nucleus $\langle H_z \rangle$ is uniquely determined from this experiment according to the relation

$$A = -\frac{1}{IJ} \mu_I \langle H_z \rangle$$

However, the electric quadrupole field q_J can be gotten from B according to the relation $B = -e^2 q_J Q$, where Q is the spectroscopic quadrupole moment, and $q_J = \langle 3 \cos^2 \theta - 1 \rangle_{J, m_J=J} \langle 1/r^3 \rangle$. Since Q is unknown the experiments give no information about q_J .

It is well known that for a half-filled closed shell coupling to the Hund's-rule state, both $\langle H_z \rangle$ and q_J are zero if relativity is neglected. We have examined in detail three sources which could contribute to the fields. (1) Breakdown of L-S coupling within the configuration $(5d)^5(6s)^2$. (2) Admixture of the configuration $(5d)^6(6s)$ into the ground state. (3) Relativistic effects. In order to calculate these effects, a reliable wave function is needed for the ground state. Fortunately Trees² has analyzed the optical spectrum of rhenium and has expressed the energy levels in terms of the L-S eigenstates of the configuration $(5d)^5(6s)^2$ and $(5d)^6(6s)$. The wave function of the ground state expressed in terms of these eigenstates is

$$\Psi(J = \frac{5}{2}) = \sqrt{0.874} |^6S\rangle - \sqrt{0.108} |^4P\rangle + \sqrt{0.006} |^4D\rangle + \sqrt{0.003} |(4^3P)^4Pd^6s\rangle \\ - \sqrt{0.005} |^5^2D\rangle - \sqrt{0.003} |^1^2D\rangle + \sqrt{0.001} |^3^2F\rangle$$

The calculation of the fields at the nucleus may be performed by first expanding the wave function into single-particle coordinates according

to the notation of Condon and Shortley.¹⁰ In this notation the $6S_{5/2}$ level is written as $2^+ 1^+ 0^+ -1^+ -2^+$, for example. The evaluation of the fields at the nucleus then proceeds in a manner similar to that shown previously for Am²⁴¹, and the reader is referred to the Am paper for details.¹¹ It is essential in this calculation to assure that our notation for the states is consistent with the phases of Trees. To do this we have used first-order perturbation theory to calculate the phases of the admixing coefficients (see reference 11 for details) and have chosen the phases so that agreement with Trees is obtained. This procedure is reliable, since the coefficients are quite small.

There are two parameters relating to the radial wave functions that require evaluation. One needs to know $\langle 1/r^3 \rangle_{5d}$ and $|\Psi(0)|_{6s}^2$. We have evaluated these quantities in the following way. Cohen has produced Hartree-Fock solutions to the Dirac equation for the ground states of tungsten ($Z = 74$) and of platinum ($Z = 78$).¹² The radial functions are available for $5d_{3/2}$ and have been used to evaluate the dipole and quadrupole $\langle 1/r^3 \rangle$'s from the relations

$$\langle 1/r^3 \rangle_{5d}^{\text{dipole}} = \frac{2}{\alpha a_0 (\ell+1)} \int_0^\infty \frac{FG}{r^2} dr,$$

$$\langle 1/r^3 \rangle_{5d}^{\text{quadrupole}} = \int_0^\infty \frac{F^2 + G^2}{r^3} dr.$$

These values are given in Table II. To find the values appropriate to rhenium, we have performed a linear interpolation. An approximately linear interpolation has recently been used with much success in predicting many of the properties of rare earth atoms and ions.¹³ The value of $|\Psi(0)|_{6s}^2$ was determined from the optical data of Schuler and Korsching.¹⁴

These workers measured the hyperfine structure in the states $^8P_{7/2}$ and $^8P_{5/2}$ arising from the configuration ($d^5 sp$) of Re^{187} . The values obtained are $A(^8P_{7/2}) = 113.46 \text{ mK}$ and $A(^8P_{5/2}) = 109.96 \text{ mK}$. To determine a_{6s} we have used a model for the coupling in which d^5 couples to $^6S_{5/2}$ and $^6S_{5/2}$ couples with $6s$ to 7S_3 . This then couples with $p_{1/2}$ in j-j coupling to give the observed states. From this model we predict $A(^8P_{7/2}) = A(^8P_{5/2}) = \frac{1}{7} a_{6s}$, giving for $a_{6s} \approx 0.8 \text{ mK}$. Although this model is admittedly naive we have tried other assumptions for the coupling, always obtaining about the same result. We believe the value for a_{6s} to be relatively independent of the coupling. In addition we have calculated a_{6s} from Cohen's integrals for $6s_{1/2}$, using the expression

$$|\Psi(0)|_{6s}^2 = -\frac{1}{\pi a_0} \int_0^\infty \frac{FG}{r^2} dr.$$

These values are also shown in Table II. When Cohen's expressions are used along with the known nuclear moment of Re^{187} , we obtain $a_{6s} = 0.7 \text{ mK}$. This is in good agreement with the value obtained from Schuler and Korsching. The large value of $|\Psi(0)|_{6s}^2$ relative to $\langle 1/r^3 \rangle_{5d}$ should be noted. This is typical, and is confirmation of the fact that small amounts of configuration mixing involving unpaired s electrons can give large contributions to the hyperfine structure. The magnitude of the contributions to the hyperfine structure is shown in Table III.

Although the magnetic dipole hfs is of the right magnitude to explain the experimental result, it seems to be of the wrong sign. Accordingly, it seems reasonable to assume that the dipole field predicted from the Trees wave function is also of the wrong sign, and to look for other contributions. We are therefore led to consider relativistic effects. We show that they reverse the sign of the dipole field and largely cancel the quadrupole field.

In order to calculate relativistic effects in a complex atom the following relativistic matrix elements are needed:

$$\langle \ell s m_\ell m_s | H_z | \ell s m_\ell m_s \rangle = eC_1^2 \left(\frac{2m(\ell+1)}{(\ell+\frac{1}{2})(\ell+\frac{3}{2})} \right) \int_0^\infty \frac{F_+ G_+}{r^2} dr - eC_2^2 \left(\frac{2m\ell}{(\ell-\frac{1}{2})(\ell+\frac{1}{2})} \right) \\ \times \int_0^\infty \frac{F_- G_-}{r^2} dr - eC_1 C_2 \frac{2}{2\ell+1} [(\ell+m+\frac{1}{2})(\ell-m+\frac{1}{2})]^{\frac{1}{2}} \int_0^\infty \frac{F_+ G_- + F_- G_+}{r^2} dr,$$

where H_z is the magnetic field operator, and

$$\langle \ell s m_\ell m_s | \frac{1}{r^3} (3 \cos^2 \theta - 1) | \ell s m_\ell m_s \rangle \\ = C_1^2 \left[-\frac{1}{2} \frac{3m^2 - (\ell+\frac{1}{2})(\ell+\frac{3}{2})}{(\ell+\frac{1}{2})(\ell+\frac{3}{2})} \right] \int_0^\infty \frac{F_+^2 + G_+^2}{r^3} dr \\ + C_2^2 \left[-\frac{1}{2} \frac{3m^2 - (\ell-\frac{1}{2})(\ell+\frac{1}{2})}{(\ell-\frac{1}{2})(\ell+\frac{1}{2})} \right] \int_0^\infty \frac{F_-^2 + G_-^2}{r^3} dr \\ - 2C_1 C_2 \frac{12m[(\ell+\frac{1}{2}+m)(\ell+\frac{1}{2}-m)]^{\frac{1}{2}}}{(2\ell-1)(2\ell+1)(2\ell+3)} \int_0^\infty \frac{F_+ F_- + G_+ G_-}{r^3} dr.$$

Here C_1 and C_2 are the Clebsch-Gordan coefficients in the expansion

$$| \ell s m_\ell m_s \rangle = C_1 | \ell, s, j=\ell+\frac{1}{2}, m=m_\ell+m_s \rangle + C_2 | \ell, s, j=\ell-\frac{1}{2}, m=m_\ell+m_s \rangle.$$

The charge on the electron is $-e$, and F_\pm are the small and G_\pm the large components of the Dirac equation for $j = \ell \pm \frac{1}{2}$. The phase convention of Edmonds has been used. ¹⁵

In Table III we tabulate the most important contributions to the hfs. Interestingly, there is a large contribution to the dipole effect coming from ${}^6S_{5/2}$, although it is still zero for the quadrupole interaction. This occurs because the dipole interaction mixes the large and small components, whereas

the quadrupole interaction operates on the large and small components separately. Accordingly, the largest relativistic contribution to the quadrupole field comes from the off-diagonal element $\langle {}^6S_{5/2} | q_J | {}^4P_{5/2} \rangle$. In evaluating the radial integrals entering the relativistic calculation we were handicapped by the fact that there are no calculations of the $5d_{5/2}$ wave functions for tungsten. This was compensated for by scaling down the platinum integrals by the same factor as was used for the $5d_{3/2}$ integrals. These are given also in Table II.

We have made calculations to see if these results are consistent with the apparently small value for the hyperfine anomaly. To determine this, we have used the model of Bohr and Weisskopf to estimate the nuclear size effect.¹⁶ These authors give an expression for the size of the anomaly in terms of the orbital and spin g factors and the fractions of the magnetic moment arising from spin and orbital motion. Using values for these quantities obtained from the Nilsson wave functions (see next section), we find ${}^{186}\Delta^{188} = 0.18\%$. This is consistent in sign and magnitude with our result.

The total contribution to the hyperfine structure is given in Table III. It is seen that good agreement with the measured A value is obtained. The quadrupole field arises from a cancellation of the nonrelativistic and relativistic parts. A value of $Q = 1.7$ barns would be obtained for the quadrupole moment. From the collective model this would imply an intrinsic quadrupole moment $Q_0 = 10 Q = 17$ barns. This is considerably larger than would be predicted by assuming a deformation parameter $\delta \approx 0.2$ and using $Q_0 = \frac{4}{5} Z \delta R_0^2 = 6.0$ barns. A Sternheimer anti-shielding factor¹⁷ $R = -0.51$ has been calculated for $(5d)^4$ in tungsten and might apply here, or perhaps inaccuracies in the matrix elements might explain the discrepancy.

The excellent agreement of our theoretical results with the measured dipole constant and anomaly leads us to believe that our model is probably correct and that the Cohen wave functions give a good measure of the relativistic corrections for 5d electrons. We have also evaluated the relativistic corrections, using the correction factors of Casimir.¹⁸ For the value of Z_{eff} for d electrons we have chosen $(Z - 11)$ or $Z_{\text{eff}} = 64$, and the $\langle 1/r^3 \rangle_{5d}$ is the same as used in the calculation of the nonrelativistic hfs. The hfs computed in this way is too small by a factor of four to explain the effect. Schwartz¹⁹ showed that although the Casimir factors agreed with results for p electrons based on a Thomas-Fermi potential, the agreement was probably fortuitous. Recently, the relativistic corrections in europium were calculated for 4f electrons and the results of Casimir were shown to be too small by an order of magnitude.²⁰ Our result is, therefore, not surprising, and we feel justified in concluding that the Casimir correction factors are too small for 5d electrons to give reliable results.

NUCLEAR STRUCTURE

Mottelson and Nilsson²¹ have calculated equilibrium values of the deformation parameter δ for odd-A nuclei in the region $151 < A < 195$, using the collective model with a harmonic oscillator single-particle potential. Experimental values of δ were then obtained from values of Q_0 based on observed E2 transition probabilities. Agreement between calculated and measured δ 's for both odd-A and even-even nuclei is good over most of the region, particularly for ${}_{74}\text{W}$ and ${}_{76}\text{Os}$.

The predicted value of δ for ${}_{75}\text{Re}$ is 0.19, which agrees favorably with the value 0.22 obtained from the measured quadrupole moment of Re^{185} . This δ and the measured ground-state spins of $5/2+$ for both Re^{185} and Re^{187} led to the assignment of $[402]5/2$ to the 75th proton.

Because both Re^{186} and Re^{188} have $I = 1-$, the 111th and 113th neutrons have been assigned to the $[512]3/2$ state. This assignment fits the Mottelson-Nilsson energy level diagram exactly if $\delta_{186} > 0.22$, $0.19 < \delta_{188} < 0.22$. The ordering $\delta_{188} < \delta_{186}$ is supported by the results of our experiment. The quadrupole constants B are a measure of the deformation, and $B_{188} < B_{186}$ implies that $\delta_{188} < \delta_{186}$. For the proposed state assignments, an increasing nuclear moment implies smaller deformation (see Table IV). Therefore, the results $\mu_I(188) > \mu_I(186)$ supports the conclusion $\delta_{188} < \delta_{186}$.

The magnetic moment μ_I has been calculated with these state assignments and the wave functions of Nilsson and Mottelson. The calculation was done for various positive values of δ , using both free-nucleon g factors and the quenched g factors ($g_{sp} = 4.0$, $g_{sn} = -2.4$) suggested by Chiao and Rasmussen.²² The results are shown in Table IV. The value Z/A was used for the core g factor, g_R . Chiao has suggested, on the basis of different pairing energies for neutrons and protons, that g_R for odd-odd nuclei should be $g_R = (3/4)Z/A$. If this were done, each of the results in Table IV would be lowered by 0.05 nm.

It is seen from Table IV that with quenched g factors, $\mu_I(188)$ is predicted very well by a deformation of 0.2, and $\mu_I(186)$ by a deformation of slightly less than 0.3. This is in good agreement with the deformations assumed.

REFERENCES

1. Charlotte E. Moore, Atomic Energy Levels (National Bureau of Standards, Washington, D. C., 1958), Vol. 111, NBS-467.
2. R. E. Trees, Phys. Rev. 112, 165 (1958).
3. Walter M. Doyle and Richard Marrus, Nucl. Phys. 49, 449 (1963).
4. R. G. Schlecht, M. B. White, and D. W. McColm, Hyperfine Structures of Re¹⁸⁶ and Re¹⁸⁸ (to be submitted to Physical Review).
5. D. Strominger, J. M. Hollander, and G. T. Seaborg, Rev. Mod. Phys. 30, No. 2 part 2, 585 (1958).
6. R. Winkler, D. Naturwiss. 10, 236 (1964).
7. W. A. Nierenberg, Ann. Rev. Nucl. Sci. 7, 349 (1957).
8. W. A. Nierenberg and G. O. Brink, J. Phys. Radium 19, 816 (1958); P. G. H. Sandars and G. K. Woodgate, Nature 181, 1395 (1958).
9. Hans Kopfermann, Nuclear Moments, English Version by E. E. Schneider (Academic Press, Inc., New York, 1958).
10. E. U. Condon and G. H. Shortley, Theory of Atomic Structure (Cambridge University Press, Cambridge, England, 1957).
11. Richard Marrus, William A. Nierenberg, and Joseph Winocur, Phys. Rev. 120, 1429 (1960).
12. Stanley Cohen, Relativistic Self-Consistent Calculation for the Normal Tungsten Atom, Lawrence Radiation Laboratory Report UCRL-8634, April 1959 (unpublished); Relativistic Self-Consistent Calculation for the Normal Platinum Atom, Lawrence Radiation Laboratory Report UCRL-8635, April 1959 (unpublished).
13. B. R. Judd and I. Lindgren, Phys. Rev. 122, 1802 (1961).

14. H. Schuler and H. Korsching, Z. Physik 105, 168 (1937).
15. A. R. Edmonds, Angular Momentum in Quantum Mechanics (Princeton University Press, Princeton, New Jersey, 1960).
16. A. Bohr and V. F. Weisskopf, Phys. Rev. 77, 94 (1950).
17. R. M. Sternheimer, Phys. Rev. 80, 102 (1950); 84, 244 (1951); 95, 736 (1954); 105, 158 (1957).
18. H. B. G. Casimir, On the Interaction Between Atomic Nuclei and Electrons (Teyler's Tweede Genootschap, Haarlem, 1936).
19. C. Schwartz, Phys. Rev. 105, 173 (1957).
20. Quoted by B. Bleaney as private communication from P. G. H. Sandars.
21. B. R. Mottelson and S. G Nilsson, Kgl. Danske Videnskab. Selskab, Mat.-Fys. Skrifter 1, 8 (1959).
22. J. O. Rasmussen and L. W. Chiao, in Proceedings of the International Conference on Nuclear Structure, Kingston, Canada, 1960, edited by D. A. Bromley and E. W. Vogt (University of Toronto Press, Toronto, 1960), p. 646; Lung-wen Chiao, The Magnetic Properties of Deformed Nuclei (Ph. D. Thesis), Lawrence Radiation Laboratory Report UCRL-9648, April 1961 (unpublished).

Table I

Re ¹⁸⁶ Data Fit	
A = - 78.3060(.0010) Mc	$g_J = - 1.951988(39)$
B = + 8.3595(16) Mc	$g_I \times 10^4 = 9.341(23)$

Transition				H	Frequency	Residual
F	m_F	F'	m'_F	(gauss)	(Mc/sec)	(Mc/sec)
7/2	1/2 ↔	5/2	-1/2	199.9229	24.735(5)	0.0002
3/2	-3/2 ↔	5/2	-1/2	299.8773	16.647(6)	0.002
3/2	-1/2 ↔	5/2	1/2	299.9612	59.380(5)	0.008
7/2	1/2 ↔	5/2	-1/2	299.8598	3.169(4)	- 0.003
3/2	-1/2 ↔	5/2	1/2	399.7824	54.343(4)	- 0.001
3/2	-3/2 ↔	5/2	-1/2	399.7974	22.334(4)	- 0.004
7/2	1/2 ↔	5/2	-1/2	399.8003	6.936(4)	- 0.003
3/2	-1/2 ↔	5/2	1/2	499.8241	51.064(3)	- 0.002
3/2	-3/2 ↔	5/2	-1/2	499.8241	26.026(3)	0.001

Re ¹⁸⁸ Data Fit	
A = - 80.4326(8) Mc	$g_J = - 1.952072(60)$
B = + 7.7463(11) Mc	$g_I = 9.607(.029)$

Transition				H	Frequency	Residual
F	m_F	F'	m'_F	(gauss)	(Mc/sec)	(Mc/sec)
7/2	1/2 ↔	5/2	-1/2	99.9675	92.755(3)	- 0.0004
3/2	-1/2 ↔	5/2	1/2	299.8889	61.835(1)	0.0003
3/2	-3/2 ↔	5/2	-1/2	299.8819	15.895(2)	0.001
7/2	1/2 ↔	5/2	-1/2	299.8714	3.938(1)	0.00008
3/2	-3/2 ↔	5/2	-1/2	399.7780	21.837(2)	0.0002

Fit to the observed triple resonances according to the Hamiltonian

$$A\vec{I} \cdot \vec{J} + B \frac{1}{2IJ(2I-1)(2J-1)} [3(\vec{I} \cdot \vec{J})^2 + 3/2(\vec{I} \cdot \vec{J}) - I(I+1)J(J+1)] - g_J \mu_0 \vec{J} \cdot \vec{H} - g_I \mu_0 \vec{I} \cdot \vec{H}$$

Table II. Numerical parameters (in units of a_0^{-3}).

	W	Pt	Re
$\langle 1/r^3 \rangle_{5d}^{\text{dipole}}$	4.7	10.0	6.0
$\langle 1/r^3 \rangle_{5d}^{\text{quadrupole}}$	5.1	11.1	6.6
$ \Psi(0) _{6s}^2$	19.7	24.7	20.9
$e \int_0^\infty \frac{F_- G_-}{r^2} dr$	$14.0 \mu_0$	$29.7 \mu_0$	$17.9 \mu_0$
$e \int_0^\infty \frac{F_+ G_+}{r^2} dr$	---	$-16.0 \mu_0$	$-9.6 \mu_0$
$e \int_0^\infty \frac{F_+ G_- + F_- G_+}{r^2} dr$	---	$8.6 \mu_0$	$5.2 \mu_0$
$\int_0^\infty \frac{F_-^2 + G_-^2}{r^3} dr$	5.1	11.1	6.6
$\int_0^\infty \frac{F_+^2 + G_+^2}{r^3} dr$	---	8.3	5.0
$\int_0^\infty \frac{F_+ F_- + G_+ G_-}{r^3} dr$	---	9.0	5.4

These are evaluated from Cohen's wave functions in the case of W and Pt.

The values for Re are obtained by linear interpolation.

Table III. Contribution to the hyperfine constants
A and B in rhenium.

Source	Magnitude	
	A (Mc/sec)	B (Mc/sec)
Breakdown of L-S coupling within $(5d)^5(6s)^2$	$33.6 \mu_I^a$	$+ 33.0 Q^b$
Configuration mixing $(5d)^6(6s)$	$11.2 \mu_I$	$- 0.3 Q$
Relativistic corrections	$- 83.5 \mu_I$	$- 28.0 Q$
Total calculated	$- 38.7 \mu_I$	$4.7 Q$
Total experimental	$- 46.0 \mu_I$	8.0

^a μ_I in nm.

^b Q in barns.

Table IV. Nuclear moments calculated with Nilsson wave functions.

	η		
	<u>2</u>	<u>4</u>	<u>6</u>
Free nucleon g factors	2.11	1.92	1.84
Quenched nucleon g factors	1.89	1.77	1.72

Proton state $[402\uparrow](5/2+)$. Neutron state $[512\downarrow](3/2-)$.

FIGURE CAPTIONS

Fig. 1. Schematic representation of the hairpin arrangement for triple resonance experiment.

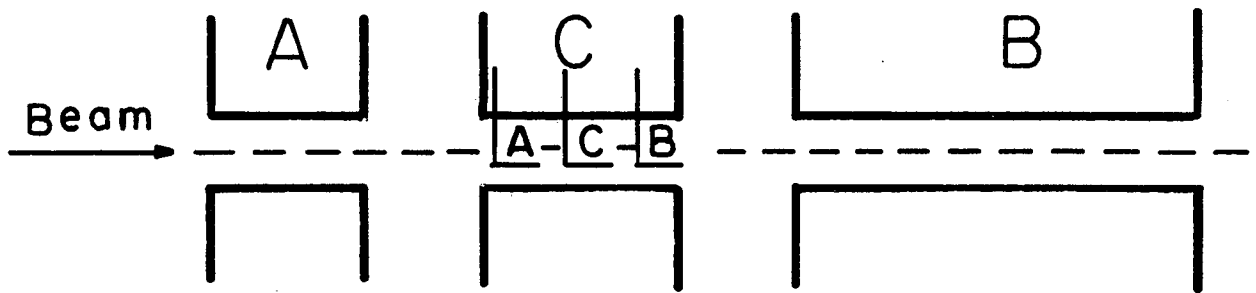
Fig. 2. Some observed triple resonance lines.

(a) Re^{186} ; $H_0 = 500 \text{ g}$; $(5/2 \quad 1/2) \leftrightarrow (3/2 \quad 3/2)$

(b) Re^{186} ; $H_0 = 300 \text{ g}$; $(5/2 \quad -1/2) \leftrightarrow (3/2 \quad 1/2)$

(c) Re^{188} ; $H_0 = 300 \text{ g}$; $(7/2 \quad -1/2) \leftrightarrow (5/2 \quad 1/2)$

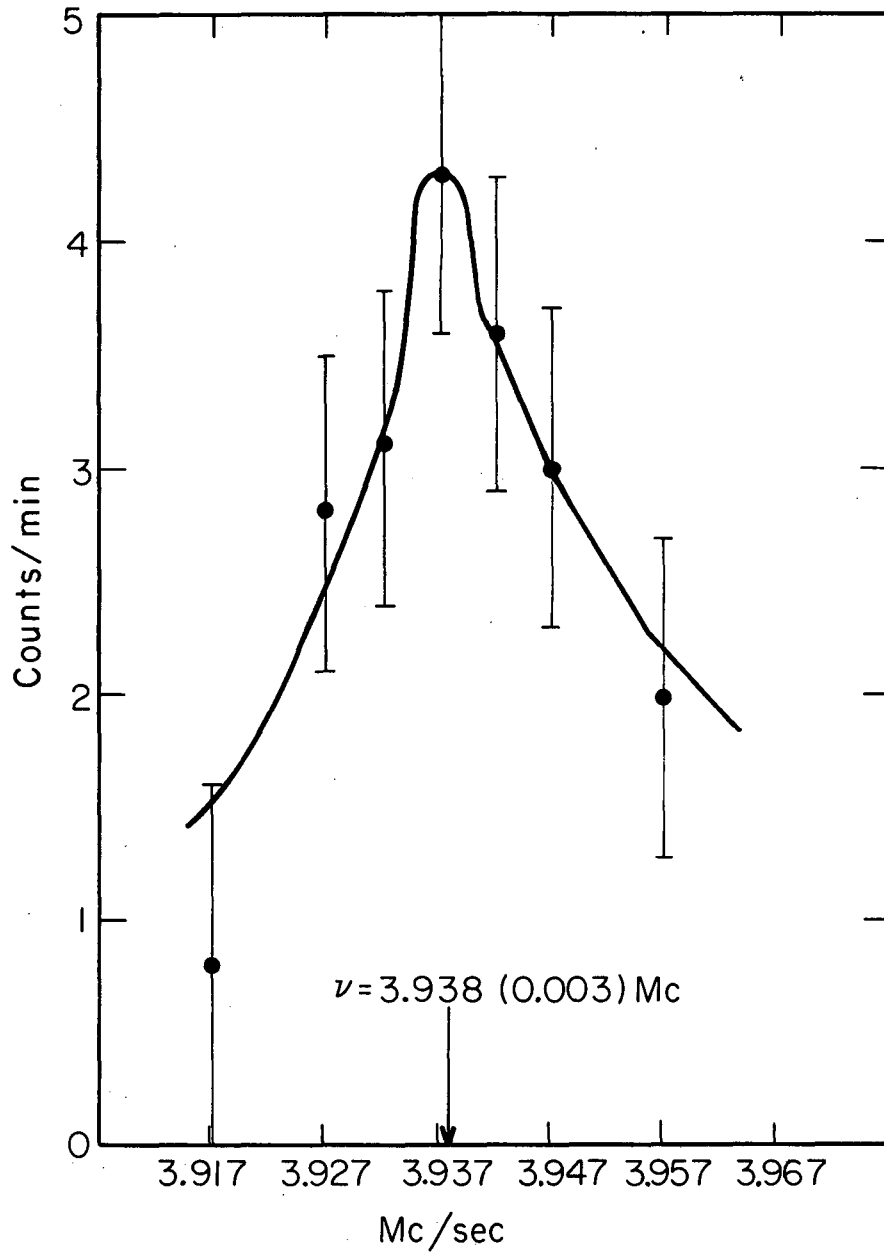
Fig. 3. Breit-Rabi diagram for $I = 1$, $J = 5/2$.



Schematic of magnets and hairpins

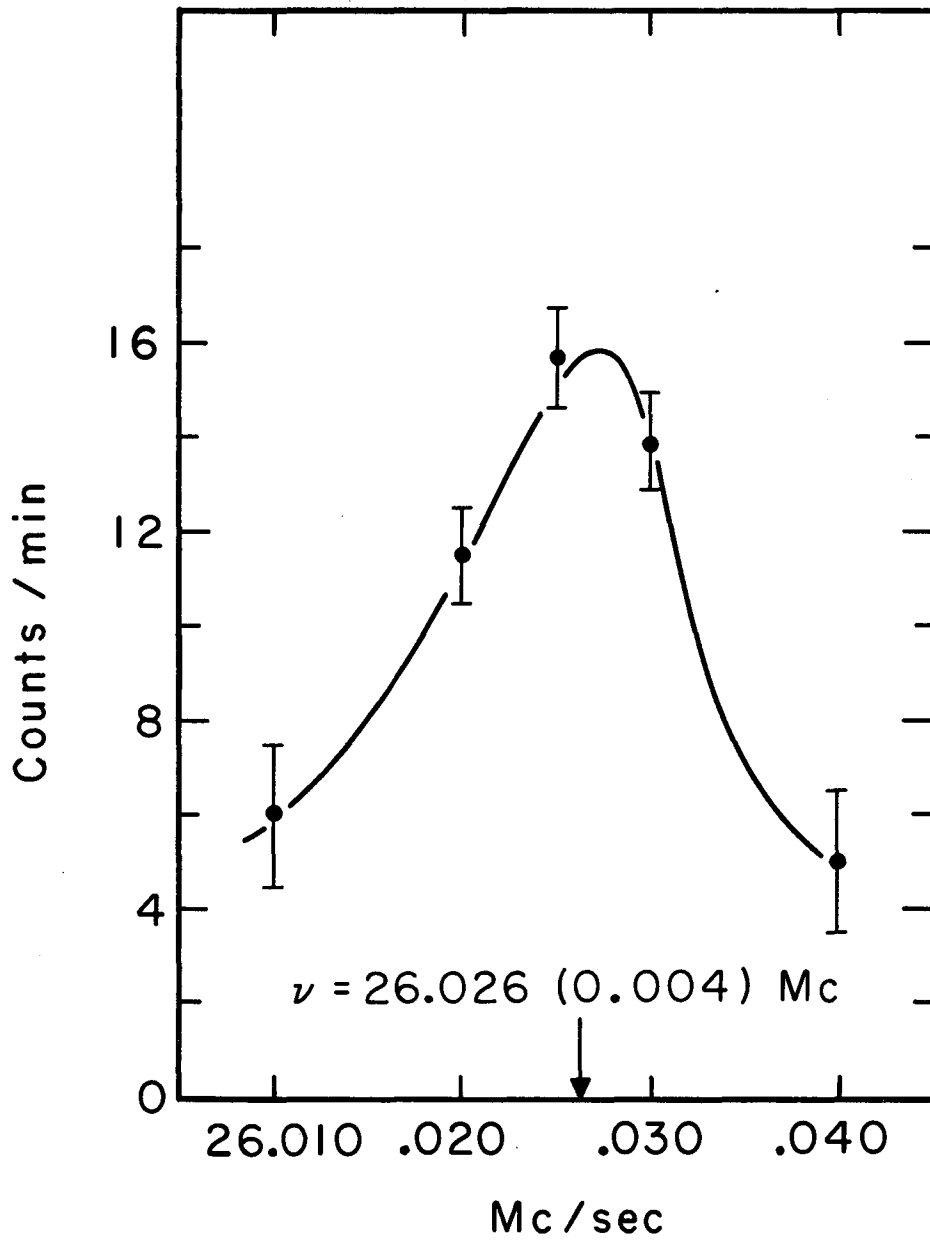
MUB-4246

Fig. 1



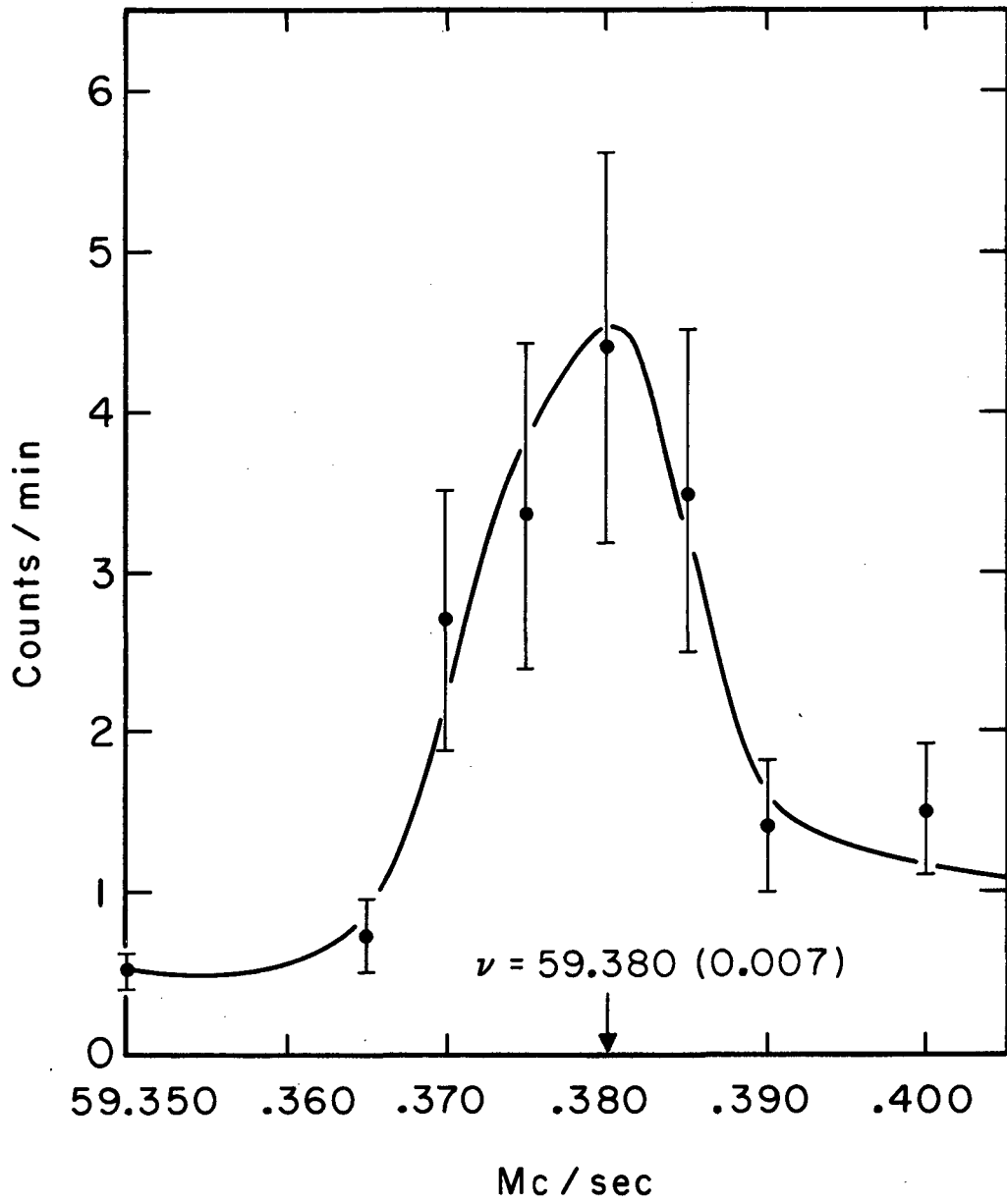
MUB-4247

Fig. 2a



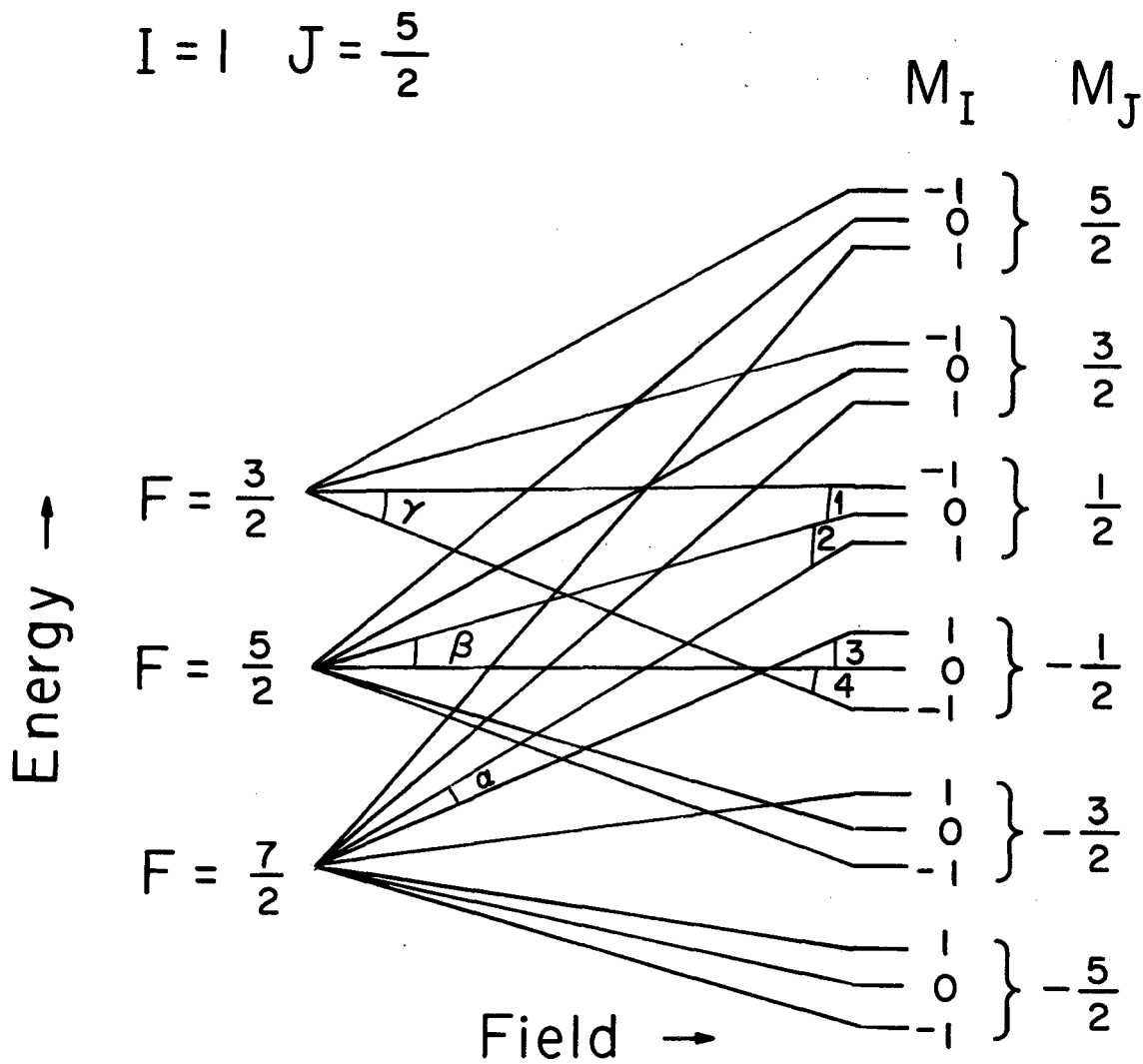
MUB-4556

Fig. 2b



MUB-4557

Fig. 2c



MUB-4244

Fig. 3

This report was prepared as an account of Government sponsored work. Neither the United States, nor the Commission, nor any person acting on behalf of the Commission:

- A. Makes any warranty or representation, expressed or implied, with respect to the accuracy, completeness, or usefulness of the information contained in this report, or that the use of any information, apparatus, method, or process disclosed in this report may not infringe privately owned rights; or
- B. Assumes any liabilities with respect to the use of, or for damages resulting from the use of any information, apparatus, method, or process disclosed in this report.

As used in the above, "person acting on behalf of the Commission" includes any employee or contractor of the Commission, or employee of such contractor, to the extent that such employee or contractor of the Commission, or employee of such contractor prepares, disseminates, or provides access to, any information pursuant to his employment or contract with the Commission, or his employment with such contractor.

